Characterization of the Structures of Phosphodiesterase 10 Binding with Adenosine 3′,5′-Monophosphate and Guanosine 3′,5′-Monophosphate by Hybrid Quantum Mechanical/Molecular Mechanical Calculations

Haiting Lu,[†,‡] Alan C. Goren,[‡,§] and Chang-Guo Zhan*[,‡]

College of Chemistry and Chemical Engineering, Xinyang Normal University, Xinyang 464000, P. R. China, Department of Pharmaceutical Sciences, College of Pharmacy, University of Kentucky, 725 Rose Street, Lexington, Kentucky 40536 and Division of Natural Sciences & Mathematics, Transylvania University, 300 North Broadway, Lexington, Kentucky 40508

Received: December 4, 2009; Revised Manuscript Received: April 18, 2010

Quantum mechanical/molecular mechanical (QM/MM) geometry optimizations of the X-ray crystal structures of PDE10−AMP (PDB code 2OUN) and PDE10−GMP (PDB code 2OUQ) complexes have been performed to characterize the state of the AMP and GMP products, respectively. Results show that only one phosphate oxygen atom (O1) is protonated for both AMP and GMP product complexes. In addition, QM/MM calculations have resolved the orientation of the amide group of Gln726 in PDE10−GMP which was in conflict with the assignment of the guanine group of GMP in the X-ray crystal structure. Calculations reveal that the amide oxygen and nitrogen atom of Gln726 are rotated 180°, resulting in two strong hydrogen bonds formed between the amide group of Gln726 and the guanine group of GMP. Binding free energy calculations for both QM/MM-optimized structures confirm the new conformational assignment of Gln726 in PDE10−GMP. The calculated binding free energy of the rotated structure is ∼22 kcal/mol lower than the X-ray crystal assignment. The lower energy is mainly derived from the formation of two hydrogen bonds between the amide group of Gln726 and the guanine group of GMP. This implies that the orientation of the amide oxygen and nitrogen atoms in PDE10−AMP is different from PDE10−GMP. Finally, our results help to understand why PDE10 can hydrolyze both cAMP and cGMP.

Introduction

Cyclic nucleotide phosphodiesterases (PDE's) regulate physiological processes by degrading intracellular secondary messengers cyclic adenosine 3′,5′-monophosphate (cAMP) or cyclic guanosine 3′,5′-monophosphate (cGMP) to 5′-nucleotide monophosphates AMP or GMP through PDE-catalyzed hydrolysis.[1−9] PDEs constitute a large superfamily (with at least 11 different gene families, i.e., PDE1−PDE11) of structurally related, functionally distinct, and highly regulated enzymes.[10] There are three catagories related to the substrate specificity of PDE's: cAMP-specific enzymes (PDE4, PDE7, and PDE8), cGMP-specific enzymes (PDE5, PDE6, and PDE9), and the dual specificity (PDE1, PDE2, PDE3, PDE10, and PDE11). Most cells contain representatives of multiple PDE gene families but in different amounts, proportions, and subcellular locations. For example, PDE3A is highly expressed in cardiac muscle, vascular and visceral smooth muscle, and platelets, whereas PDE3B, the product of a distinct gene, is expressed in adipocytes, hepatocytes, spermatocytes, and renal collecting duct epithelium.[11] PDE4 is mainly expressed in inflammatory cells and central neurons. PDE5 isomers are relatively abundant in vascular smooth muscle, including the pulmonary vasculature and corpus cavernosum of the penis.[12] PDE10 was first reported by three groups in 1999.[13−15] This enzyme is highly expressed in the central nervous cystem (CNS), making it an important target for therapeutic approaches for the treatment of psychoses.[16−18] Consequently, different families of PDE's are potential drug targets for the treatment of different diseases.

Crystal structures for the catalytic domains of nine different PDE families have been solved over the past few years. In 2007, Ke et al.[19] first published eight X-ray crystal structures of the catalytic domain of the wild-type and mutated PDE10A2 including complexes with products AMP and GMP. The binding modes of AMP and GMP in the active site of PDE10 are very similar except for the hydrogen-bonding mode between the amide group of Gln726 and the adenine or guanine group of products AMP and GMP, respectively.

In the present computational study, we mainly focused on the crystal structures of PDE10 with its two products (AMP and GMP) and examined the detailed binding interactions of the enzyme−product complexes. As the structures of the products AMP and GMP are similar to those the substrates cAMP and cGMP, respectively, a detailed structural understanding of the enzyme−product complexes should be valuable for understanding the detailed structures of the enzyme−substrate complexes and the catalytic mechanisms of PDE10.

The catalytic domain of PDE10 adopts a compact structure consisting of 15 α-helices without β-sheets. The crystal structures show that the overall topology is very similar with other known structures of PDE families. The two metal ions in the active site were assigned as Zn(II) and Mg(II). In both PDE10−AMP and PDE10−GMP complexes, Zn(II) ion was coordinated to His529, His563, Asp564, Asp674, and two phosphate oxygen atoms (O1 and O3). Mg(II) was coordinated to Asp564, two phosphate oxygen atoms (O2 and O3), and three

* To whom correspondence should be addressed. Phone: 859-323-3943. Fax: 859-323-3575. E-mail: zhan@uky.edu.
† Xinyang Normal University.
‡ University of Kentucky.
§ Transylvania University.

10.1021/jp911527y
Published on Web 05/05/2010

CHART 1: Active Site Structure[a] of PDE10−GMP Complex[19]

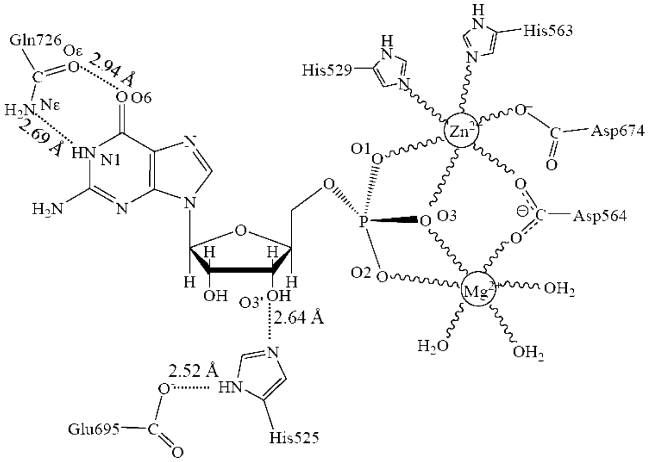

[a] Zn(II) is coordinated to His529, His563, Asp564, Asp674, and two phosphate oxygen atoms (O1 and O3); Mg(II) is coordinated to Asp564, two phosphate oxygen atoms (O2 and O3), and three water molecules. The wavy line refers to a coordination bond. There are unfavorable interactions between the GMP guanine group and the Gln726 amide group as these two groups are nearly coplanar.

water molecules. O3 acts as the bridging atom connecting two metal ions and forms one strong hydrogen bond with the Oδ atom of Asp674. Therefore, there should be one hydrogen atom between O3 and Oδ. However, it is not clear whether this hydrogen atom is on O3 or Oδ since hydrogen atoms cannot be determined by X-ray diffraction. The distance between the O3′ and the Nδ atoms of His525 is approximately 2.7 Å; thus, there should be a strong hydrogen bond between them. The hydrogen-bond donor is the hydrogen atom on O3′, which is the hydrolyzed oxygen, and the Nε atom of His525 forms a strong hydrogen bond with Glu695 as well. Therefore, in the following calculations, His525 will be assigned as HID (see Chart 1).

Two hydrogen bonds have been assigned between N1, N6 of AMP and the amide group of Gln726 in the PDE10−AMP complex. N1, as the hydrogen-bond acceptor, forms a hydrogen bond with the hydrogen atom on the amide nitrogen of Gln726, and N6, as the hydrogen-bond donor, forms a hydrogen bond with Oε in Gln726. Gln726 forms a hydrogen bond with Tyr693 and a water molecule as well. However, the orientation of the amide group of Gln726 in PDE10−GMP is the same as the PDE10−AMP complex. Comparing the adenine group of AMP and the guanine group of GMP, the hydrogen-bond character appears to be reversed. On the basis of this assignment, the hydrogen-bond donor and acceptor of the Gln726 amide group suggest severe torsional strain with the guanine group of GMP. Ke et al.[19] reported only one hydrogen bond between Gln726 and the GMP guanine group. In the X-ray crystal structure of the PDE10−GMP complex, the distance between the Nε atom of Gln726 and N1 of GMP is 2.69 Å, implying a strong hydrogen bond. However, there are two hydrogen atoms on Nε and one hydrogen atom on N1; thus, the hydrogen atoms on both nitrogen atoms exhibit steric hindrance with each other. The distance between the Oε atom of Gln726 and O6 of GMP is 2.94 Å, which is too close for two oxygen atoms without forming a hydrogen bond between them. However, if we flip the positions of the Oε and Nε atoms of Gln726, the Oε forms a hydrogen bond with the hydrogen atom on N1 and the hydrogen atom on Nε forms a hydrogen bond with O6. Notably, this rotation does not affect the hydrogen bond between Gln726 and Tyr693.

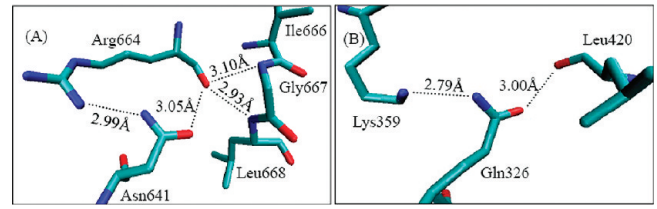

Figure 1. H-bonding interactions of the amide group of Asn/Gln in X-ray crystal structures of PDEs. (A) Amide oxygen and nitrogen atoms of Asn641 have sterically unfavorable interactions with the main chain oxygen of Arg664 which has two H bonds with backbone nitrogen atoms of Gly667 and Leu668 in PDB code 2OUQ (PDE10, resolution 1.9 Å).[19] (B) Amide oxygen and nitrogen atoms of Gln326 have sterically unfavorable interactions with the main chain oxygen of Leu420 and the ammonium ion of the side chain of Lys359 in PDB code 1ZXL (PDE7, resolution 1.67 Å).[30]

This glutamine residue (Gln726) is absolutely conserved in all PDEs families. In the X-ray crystal structures of PDE4−AMP (PDB code 1TB7) and PDE5−GMP (PDB code 1T9S) complexes, the amide oxygen and nitrogen atoms of this conserved glutamine are reversed. As a result, Zhang et al.[20] proposed the "glutamine switch" mechanism for nucleotide selectivity by phosphodiesterase, although this "glutamine switch" mechanism has been questioned by other investigators who performed mutagenesis experiments. In cGMP-specific PDE5, this glutamine (Gln817) is stabilized by Gln775 and forms two hydrogen bonds with the GMP product. When Gln817 was mutated to alanine, the mutation only weakened PDE5−cGMP binding but did not significantly affect the PDE5−cAMP binding.[21] As a result, Ke at al.[19] proposed a "substrate specificity pocket" or S-pocket mechanism in which the amino acids in the active site of PDEs and the conformation of substrates cAMP and cGMP impact substrate specificity. It is our contention that this conserved glutamine is the key residue in determining specificity in some PDE enzymes, but it is not the key element for other PDE families.

The amide groups in the side chains of asparagine (Asn) and glutamine (Gln) mostly act as hydrogen-bond donors and acceptors in the X-ray crystal structures. It is difficult to distinguish the amide nitrogen and oxygen atoms as the electron density only traces the shape of the molecules but does not clearly identify the exact atom except at an extremely high resolution. Also, the amide group of Asn and Gln may be flipped by 180° with essentially no affect on the electron density. Therefore, the positions of the amide nitrogen and oxygen atoms should be assigned based on their chemical environments, i.e., the hydrogen-bonding network around them. A number of studies over the past decade[22−26] have addressed the Asn and Gln amide assignment controversy. Approximately 20% of the current protein structure database[24,27,28] contains incorrect Asn and Gln amide rotamer assignments. In the X-ray crystal structures of known PDE families, there are many Asn/Gln amide rotamers with sterically unfavorable interactions (see Figure 1). In order to confirm the correct Gln726 amide orientation, we used two web-based services to detect incorrect Asn/Gln rotamers of the PDE10−GMP complex. First, we used Lovell's version to evaluate the X-ray crystal structure of PDE10−GMP complex by minimizing steric hindrances after adding hydrogen atoms to the enzyme system (http://molprobity.biochem.duke.edu/). The results indicated the Gln276 amide group should be flipped. In 2006, Sippl et al.[27−29] created NQ-

Flipper which is a web service to automatically detect and correct erroneous Asn/Gln amide rotamers (https://flipper.services.came.sbg.ac.at/). According to the scores obtained by NQ-Flipper, Gln726 is rated as "ambiguous" as the scores are almost identical regardless of whether or not the amide group is flipped. NQ-Flipper does not consider ligands and nonstandard groups, and scores of residues in the vicinity of nonprotein groups are unreliable. We performed various high-level QM/MM calculations in order to evaluate the Gln725 amide group and estimate the energy difference between the flipped and the nonflipped rotamers.

Computational Methods

QM/MM Calculations. All QM/MM calculations were performed using the pseudobond QM/MM method.[31,32] The pseudobond QM/MM method was initially implemented in revised Gaussian03 and Tinker programs.[31,32] In this study, we used a newly revised version[33−35] of Gaussian03 and Amber8 programs to perform the QM/MM calculations.

The initial PDE10−AMP and PDE10−GMP structures used in the paper were directly extracted from the corresponding X-ray crystal structure deposited in the Protein Data Bank (PDB codes 2OUN and 2OUQ).[19] All hydrogen atoms were added to the enzyme using the AMBER8.0 program;[36] the standard protonation states at physiological condition (pH ≈ 7.4) were set to all ionizable residues. Then the structure with all added hydrogen atoms was minimized with all the heavy atoms fixed in about 3000 steps. This minimized structure was used to prepare the input file for both the quantum mechanical and the molecular mechanics portions. The quantum part was optimized by employing density functional theory (DFT) using Becke's three-parameter hybrid exchange functional and the Lee−Yang−Parr correlation functional (B3LYP)[37−39] with the 6-31G(d) basis set[40] in Gaussian03 suite.[41] The molecular mechanics portion was calculated with all other atoms fixed 20 Å from the phosphorus atom of AMP or GMP using the AMBER8.0 program. The quantum portion contains the ligand, two metal ions, the residues coordinated to the metal ions, an additional histidine (His525), and an additional glutamate (Glu695) (see Figures 2− 4 where all QM atoms are shown as balls).

Binding Free Energy Calculations. The binding free energies between PDE10 and the ligands were calculated with quantum mechanics/molecular mechanics (QM/MM) and the Poisson−Boltzmann surface area model (PBSA). We labeled the method as QM/MM-PBSA.

In the QM/MM-PBSA method, the free energy of a ligand binding with a protein, ΔG_{bind}, is calculated from the difference between the free energy of the receptor−ligand complex (G_{cpx}) and the sum of the free energies of the unbound receptor (G_{rec}) and ligand (G_{lig}) as follows:

$$\Delta G_{bind} = (G_{cpx}) - (G_{rec}) - (G_{lig})$$

The binding free energy ΔG_{bind} was evaluated as a sum of the changes in the QM/MM gas-phase binding energy ($\Delta E_{QM/MM}$), solvation free energy (ΔG_{solv}), and entropy contribution ($-T\Delta S$).

$$\Delta G_{bind} = \Delta E_{QM/MM} + \Delta G_{solv} - T\Delta S$$

$$\Delta E_{QM/MM} = E_{QM/MM}(com) - E_{QM/MM}(rec) - E_{QM}(lig)$$

The QM/MM gas-phase binding energy $\Delta E_{QM/MM}$ is partitioned into three terms: $E_{QM/MM}$(com), $E_{QM/MM}$(rec), and E_{QM}(lig).

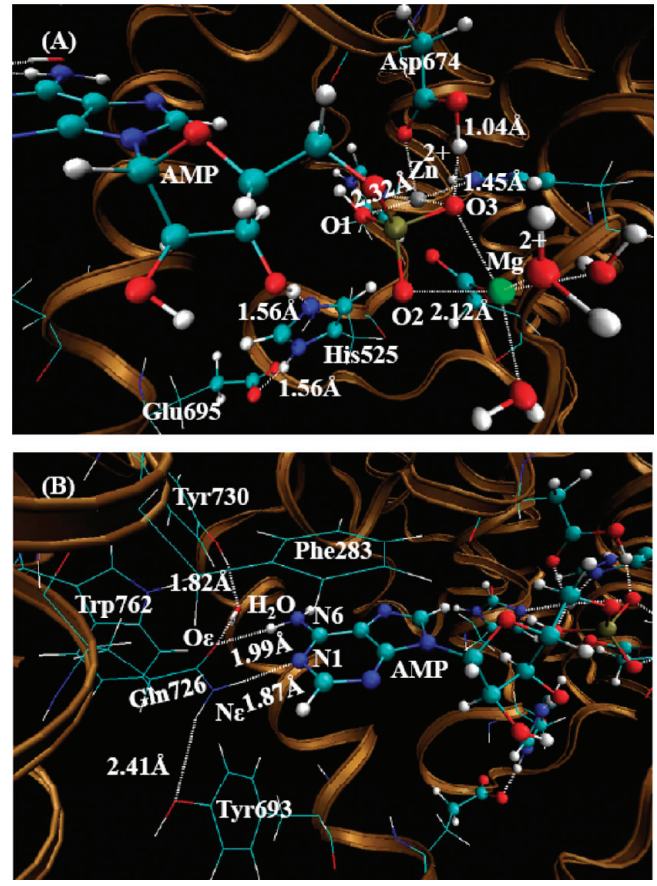

Figure 2. QM/MM-optimized PDE10−AMP structure (the charge on AMP is −1) at the B3LYP/6-31G*:Amber level. The QM atoms in the PDE10 active site are represented by balls. The lines and all other atoms represent MM atoms. (A) From this orientation, one can clearly see the metal sites and the state of AMP. (B) From this orientation, one can clearly see the hydrogen-bonded network around the Gln726 residue.

$E_{QM/MM}$(com) is calculated at the B3LYP/6-31G*:Amber level using the revised Gaussian03 and Amber8 software developed in our lab.[33,34] $E_{QM/MM}$(rec) was calculated at the same level using the QM/MM method as well. The receptor was optimized again after the ligand was deleted from the optimized complex structure. All quantum mechanical calculations contain the same atoms except the ligand atoms. For the ligand we always used the lowest energy geometry optimized at the B3LYP/6-31G* level and the corresponding energy.

$$\Delta E_{bind} = \Delta E_{QM/MM} + \Delta G_{solv}$$

$$\Delta G_{solv} = \Delta G_{PB} + \Delta G_{np}$$

$$\Delta G_{np} = \gamma SASA + \beta$$

The sum of $\Delta E_{QM/MM}$ and ΔG_{solv} is denoted by ΔE_{bind}. The solvation free energy is the sum of the electrostatic solvation free energy (ΔG_{PB}) and the nonpolar solvation energy (ΔG_{np}). ΔG_{PB} was calculated from the finite-difference solution to the Poisson−Boltzmann (PB) equation implemented in the Delphi program[42,43] by using the same RESP charges as used in the MD simulations for the receptor and the quantum mechanically calculated ESP charges for the ligands. The dielectric constants used for the solute and solvent−water were 1 and 80, respec-

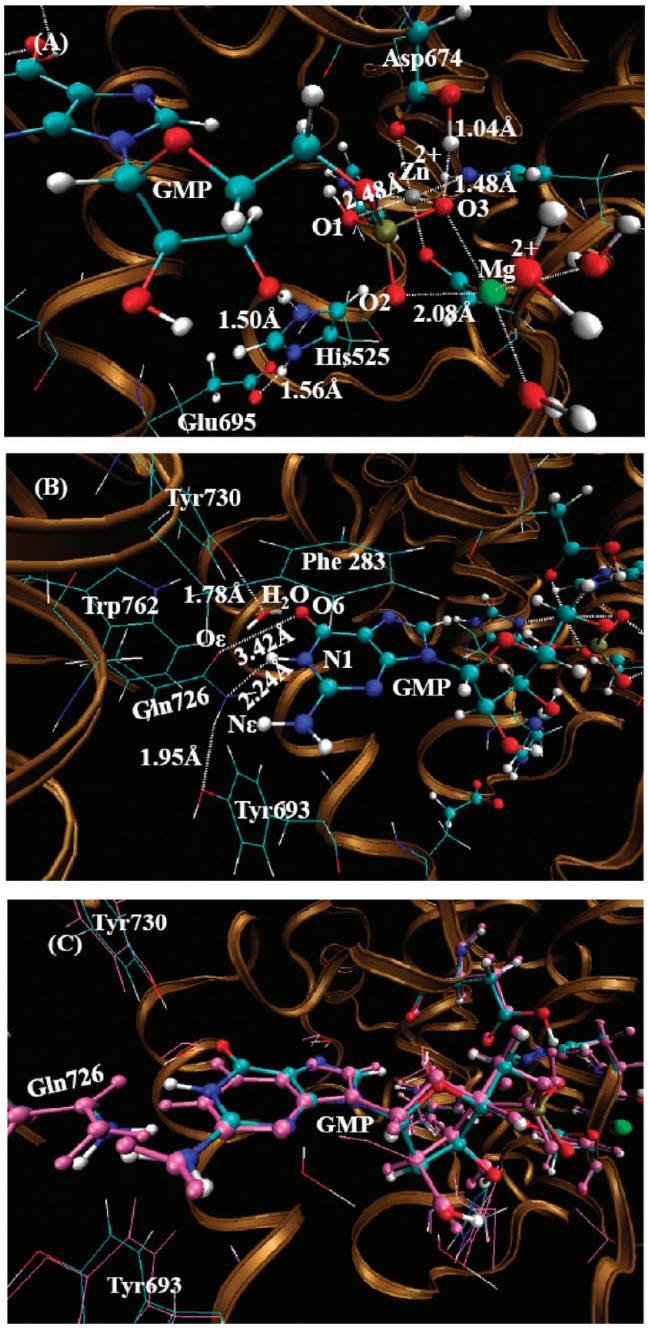

Figure 3. QM/MM-optimized PDE10−GMP structure (the charge on GMP is −1) at the B3LYP/6-31G*:Amber level. The QM atoms in the PDE10 active site are represented by balls. All MM atoms are represented as lines. (A) From this orientation, one can see the metal sites and the state of GMP. (B) From this orientation, one can see the hydrogen-bonding network around the Gln726 residue and one weak hydrogen bond between Gln726 and the guanine group of GMP. (C) Comparison between the QM/MM-optimized structure and the X-ray crystal structure while maintaining the original amide position of Gln726. The pink atoms represent the X-ray crystal structure added H atoms, and the remaining atom types represent the QM/MM-optimized structure.

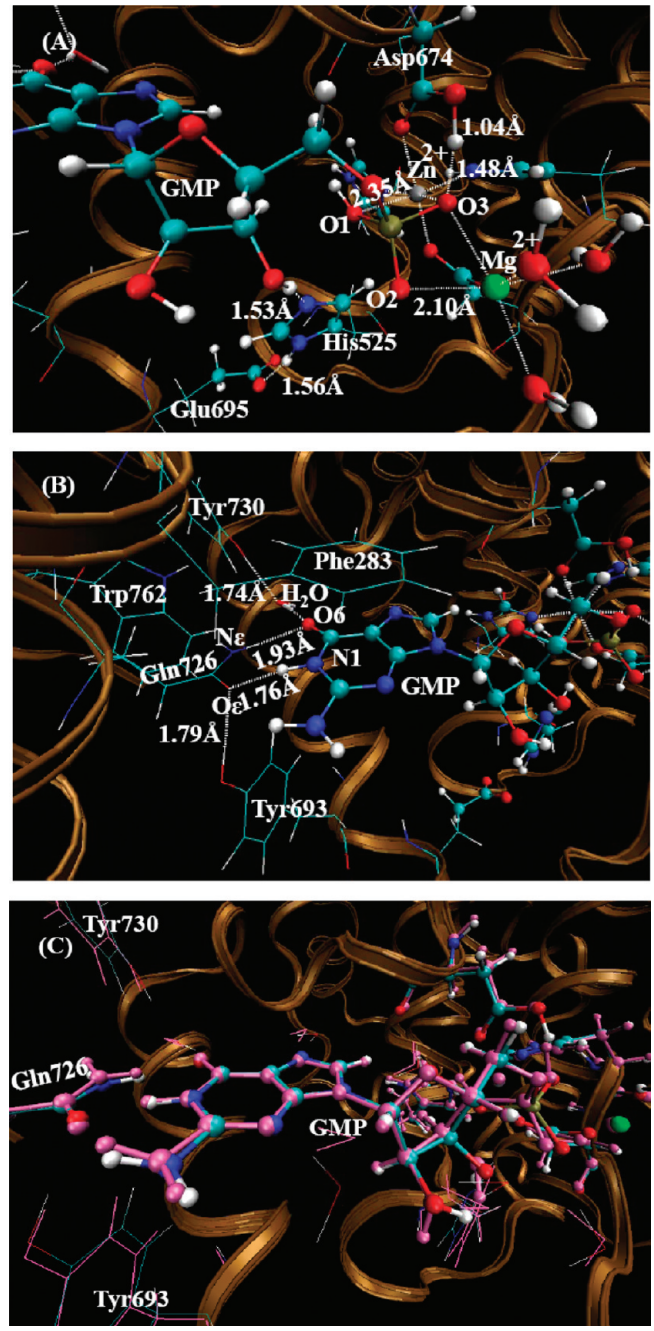

Figure 4. Geometry of the PDE10−GMP structure (the charge of GMP is −1) optimized by the QM/MM method at the B3LYP/6-31G*:Amber level. The QM atoms in the PDE10 active site are represented by balls. The lines and all other atoms represent MM atoms. (A) In this orientation, one can see the metal sites and the state of GMP. (B) In this orientation, one can see the hydrogen-bonding network around the Gln726 residue after interchange of side chain atoms and formation of two hydrogen bonds between Gln726 and the guanine group of GMP. (C) Comparison between the QM/MM-optimized structure and the X-ray crystal structure in which the amide orientation of Gln726 is changed. The pink atoms represent the X-ray crystal structure added H atoms; the atoms shown as the atom type represents the QM/MM-optimized structure.

tively. The MSMS program[44] was used to calculate the solvent-accessible surface area (SASA) from which the nonpolar solvation energy is determined using parameter values $\gamma = 0.00542$ kcal/Å^2 and $\beta = 0.92$ kcal/mol. The standard van der Waals radii built into the Amber program for solvation calculations were also used.

The entropy contribution to the binding free energy ($-T\Delta S$) was obtained by using a local program developed in our laboratory. In this method, the entropy contribution is attributed to two terms, solvation free entropy (ΔS_{solv}) and conformational free entropy (ΔS_{conf}).[45]

Results and Discussion

Depicted in Figure 2 is the QM/MM-optimized geometry of the PDE10−AMP complex with O1 protonated. In Table 1,

TABLE 1: Key Internuclear Distances[a] (Å) Involving the Metal Ions of the QM/MM-Optimized Geometries of PDE10−AMP Complex in Comparison with the Corresponding Distances in the X-ray Crystal Structure (PDB code 2OUN)[19]

internuclear distances	PDE10−AMP (O3H)[b]	PDE10−AMP (O1H,O3H)[c]	PDE10−AMP (O2H,O3H)[d]	exp
Zn(II)−O (OP-bridging)	2.718	2.526	2.663	2.457
Zn(II)−O (Asp-bridging)	2.088	2.000	2.075	2.050
Zn(II)−O (Asp−Zn)	2.042	2.148	2.133	2.074
Zn(II)−N (His1)	2.022	2.031	2.024	2.096
Zn(II)−N (His2)	2.099	2.044	2.071	2.103
Zn(II)−O (PO4)	2.084	2.319	2.085	2.371
Mg(II)−O (OP-bridging)	2.200	2.219	2.140	2.299
Mg(II)−O (Asp-briding)	2.068	2.064	2.085	2.080
Mg(II)−O (W1)	2.116	2.064	2.085	2.190
Mg(II)−O (W2)	2.079	2.053	2.090	2.121
Mg(II)−O (W3)	2.067	2.061	2.095	2.084
Mg(II)−O (PO4)	2.016	2.124	2.137	2.249
Zn(II)−Mg(II)	4.243	4.129	4.146	4.000
O3′−OP(Mg(II))	3.378	2.963	2.735	2.989
O3′−OP(Zn(II))	3.618	3.277	3.643	3.332
N6−OE1(5GP−GLN726)	2.934	3.003	2.986	3.039
N1−NE2(5GP−GLN726)	2.888	2.884	2.892	2.996
MUE (Å)[e]	0.14	0.07	0.12	

[a] The geometries were fully optimized by performing QM/MM calculations at the B3LYP/6-31G*:Amber level. [b] The charge on AMP = −1 with O3 protonated in the original file. This proton still resides on the O3 atom after QM/MM geometry optimization. [c] The charge on AMP = 0 with O1 and O3 protonated in the original file. The proton on the O3 atom migrated to the Oδ atom of Asp674 after QM/MM geometry optimization. Thus, O1 was only protonated after geometry optimization. [d] The charge on AMP = 0 with O2 and O3 protonated in the original file. The proton on the O3 atom migrated to the Oδ atom of Asp674, the proton on O2 transferred to O3′, and the proton on O3′ transferred to His525 after QM/MM geometry optimization. Therefore, no phosphate oxygen atoms are protonated, and His525 is protonated after geometry optimization. [e] The mean unsigned error between the calculated and experimental distances.

several important geometric parameters of the PDE10−AMP complex involving metal ions are included for comparison with the corresponding distances in the X-ray crystal structure.

Protonated State of AMP and GMP. The products AMP and GMP in both PDE10−AMP and PDE10−GMP complexes exhibit similar interactions with the two metal ions in the active site. Phosphate oxygen O1 coordinates only with the Zn(II) ion, and O2 coordinates with the Mg(II) ion. Phosphate oxygen O3 acts as a bridging atom connecting two metal ions and forms one strong hydrogen bond with Oδ of Asp674. This bonding arrangement implies that there must be a hydrogen atom between O3 and Oδ of Asp674. Therefore, in preparing the QM/MM calculation a hydrogen atom on O3 was added as there is no protonated aspartic acid parameter in Amber8. There are two protonated states for free AMP or GMP molecules. In state one, only one phosphate oxygen is protonated, whereas in state two, two phosphate oxygen atoms are protonated. Thus, there are three distinct QM/MM calculations according to the protonated state of AMP or GMP: (1) only O3 is protonated, (2) both O1 and O3 are protonated, and (3) O2 and O3 are protonated.

In Table 1, several important internuclear distances (Å) are reported comparing metal ions in the QM/MM-optimized geometries of the PDE10−AMP complex with the corresponding distances in the X-ray crystal structures. When O3 is protonated (the charge on AMP is −1), the mean unsigned error (i.e., the average of the absolute values of the distance errors) is 0.14 Å between the calculated distances and X-ray crystal data. Second, when O1 and O3 are both protonated, the proton on O3 migrates to the Oδ atom of Asp674, so the charge of AMP of −1 is conserved. The optimized structure is much closer to the X-ray crystal structure. The mean unsigned error is only 0.07 Å compared to the experimental data. However, when O2 and O3 are both protonated, the proton on O3 again migrates to the Oδ atom on Asp674 while the proton on the hydrolyzed O3′ atom is transferred to the Nε atom of His525, making His525 protonated, and the proton on O2 is transferred to the hydrolyzed O3′ atom. In this scenario, the charge of AMP is −2 with His525 protonated in the optimized structure. The calculated Zn(II)−O1 and Zn(II)−O3 distances are 0.2−0.3 Å longer than the corresponding experimental distances. The mean unsigned error is 0.12 Å in comparison to the X-ray crystal structure. After comparing all the optimized results, the assigned charge on AMP is −1 with O1 protonated in PDE10−AMP complex (see Figure 2). When and only when O1 is protonated, the calculated Zn(II)−O3 and Zn(II)−O1 distances are reasonably consistent with the corresponding experimental distances in the X-ray crystal structure.

Listed in Table 2 are important internuclear distances with the Gln amide group flipped (and without the Gln amide group flipped) involving the metal ions in the QM/MM-optimized geometries of the PDE10−GMP complex along with the corresponding distances in the X-ray crystal structure. When O3 is protonated with a −1 charge on GMP, the proton on O3 migrates to the Oδ atom on Asp674, resulting in the charge on GMP increasing to −2. The distance between Zn(II) ion and O3 is 2.83 Å, which is 0.6 Å longer than the experimental distance. In addition, the distance between the Zn(II) ion and O1 is 2.05 Å, which is 0.48 Å longer than the experimental distance. When O1 and O3 are both protonated, the proton on O3 migrates to the Oδ atom of Asp674, so the charge on GMP remains at −1. The optimized structure is very close to the X-ray crystal structure in terms of the key internuclear distances, i.e., the Zn(II)−O3 and Zn(II)−O1 distances. The calculated mean unsigned error is only 0.13 Å between the calculated distances and X-ray crystal data. However, when O2 and O3 are both protonated, the proton on O3 again migrated to the Oδ atom of Asp674, the proton on the hydrolyzed O3′ atom transfers to the Nε atom of His525, which makes His525 protonated, and the proton on O2 transfers to the hydrolyzed O3′ atom. As a result, the charge of GMP increases to −2 with His525 protonated in the optimized structure. After comparing all the optimized results, the charge on GMP should be −1 with O1 protonated in the PDE10−GMP complex. When O1 and O3 (or O2 and O3) are protonated, the proton on O3 also transfers to the Oδ atom of Asp674. The calculated mean unsigned error is 0.24 (0.23), 0.13 (0.22), and 0.21 (0.25) Å, respectively, for

TABLE 2: Several Important Internuclear Distances[a] (Å) Involving the Metal Ions in the QM/MM-Optimized Geometries of PDE10−GMP Complex in Comparison with the Corresponding Distances in the X-ray Crystal Structure (PDB code 2OUQ)[19]

internuclear distances	PDE10−GMP (O3H)[b]	PDE10−GMP (O1H,O3H)[c]	PDE10−GMP (O2H,O3H)[d]	exp
Zn(II)−O (OP-bridging)	2.830 (2.821)	2.310 (2.399)	2.799 (2.819)	2.227
Zn(II)−O (Asp-bridging)	2.061 (2.062)	2.005 (2.006)	2.066 (2.089)	2.052
Zn(II)−O (Asp−Zn(II))	2.120 (2.133)	2.156 (2.142)	2.130 (2.139)	2.072
Zn(II)−N (His1)	2.034 (2.023)	2.045 (2.035)	2.020 (2.013)	2.108
Zn(II)−N (His2)	2.101 (2.096)	2.036 (2.037)	2.078 (2.065)	2.108
Zn(II)−O (PO4)	2.051 (2.049)	2.502 (2.479)	2.092 (2.065)	2.532
Mg(II)−O (OP-bridging)	2.156 (2.150)	2.267 (2.245)	2.123 (2.140)	2.356
Mg(II)−O (Asp-briding)	2.098 (2.098)	2.042 (2.042)	2.071 (2.092)	2.080
Mg(II)−O (W1)	2.086 (2.083)	2.084 (2.125)	2.128 (2.132)	2.241
Mg(II)−O (W2)	2.091 (2.090)	2.084 (2.063)	2.085 (2.090)	2.271
Mg(II)−O (W3)	2.068 (2.071)	2.072 (2.079)	2.092 (2.103)	2.299
Mg(II)−O (PO4)	2.043 (2.044)	2.099 (2.084)	2.135 (2.111)	2.451
Zn(II)−Mg(II)	4.177 (4.155)	4.023 (4.064)	4.201 (4.180)	3.870
O3′−OP(Mg(II))	3.162 (3.141)	2.964 (2.901)	2.792 (2.688)	2.612
O3′−OP(Zn(II))	3.525 (3.562)	3.088 (3.088)	3.461 (3.666)	2.867
O6−NE2 (5GP−GLN726)	2.893 (3.402)	2.938 (3.419)	2.919 (3.416)	2.939
N1−OE1 (5GP−GLN726)	2.798 (2.971)	2.778 (2.992)	2.793 (3.054)	2.687
MUE (Å)[e]	0.24 (0.23)	0.13 (0.22)	0.21 (0.25)	

[a] The geometries were fully optimized by performing QM/MM calculations at the B3LYP/6-31G*:Amber level. The values outside the parentheses represent the flipped amide group of Gln726, and the values inside the parentheses represent the calculated distances when maintaining the original amide orientation of Gln726. [b] The charge on GMP = −1 with O3 protonated in the original file. This proton on O3 migrated to the Oδ atom of Asp674 after QM/MM geometry optimization. Also, there were no phosphate oxygens protonated after QM/MM geometry optimization. [c] The charge on GMP = 0 with O1 and O3 protonated in the original file. The proton on the O3 atom migrated to the Oδ atom of Asp674 after QM/MM geometry optimization. Also, only O1 was protonated after QM/MM geometry optimization. [d] The charge on GMP = 0 with O2 and O3 protonated in the original file. The proton on the O3 atom migrated to the Oδ atom of Asp674, the proton on O2 migrated to O3′, and the proton on O3′ migrated to His525 after QM/MM geometry optimization. Also, no phosphate oxygens were protonated, and His525 was protonated after QM/MM geometry optimization. [e] The mean unsigned error between the calculated and experimental distances.

those three optimized structures in comparison with experimental data. Thus, the optimized structure mirrors most closely the X-ray crystal structure, particularly for the Zn(II)−O3 and Zn(II)−O1 distances, when and only when O1 is protonated (see Figures 3 and 4).

Amide Oxygen and Nitrogen Orientation in the PDE10−GMP Complex. When the original position of the X-ray crystal structure of the amide oxygen and nitrogen atoms of the Gln726 residue for the PDE10−GMP complex were maintained, the guanine group moved up and the amide of Gln726 moved down following QM/MM optimization. As a result, the hydrogen on the amide nitrogen and the N1 atom of GMP interfere strongly with each other and the distance between the Oε atom of Gln726 and O6 of GMP is 2.94 Å, which is too close for two oxygen atoms without an intervening hydrogen bond. These two steric repulsions force the amide group of Gln726 and the guanine group of GMP to move away from each other, resulting in a change in the distance between Oε and O6 to approximately 3.4 Å relative to the original 2.94 Å distance. The distance between Nε and N1 changed to 2.99 Å compared to the original 2.69 Å distance. Figure 3C shows the comparison between the QM/MM-optimized structure and the X-ray crystal structure when the original amide position of Gln726 is maintained. One can clearly see that the amide group of Gln726 moved down and the guanine group of GMP moved up. This result implies that these four atoms could not possibly be this close to each other if the assignments from the X-ray crystal structure are maintained.

When the positions of the amide oxygen and nitrogen atoms of the Gln726 residue are interchanged and following QM/MM geometry optimization, the positions of Gln726 and the guanine group of GMP are nearly identical to the original experimental positions. In this atomic arrangement, two strong hydrogen bonds between Gln726 and the guanine group are formed and there is one hydrogen bond between Gln726 and Tyr693. Figure 4C shows the comparison between the QM/MM-optimized structure after interchange of the amide oxygen and nitrogen atoms of Gln726 with the X-ray crystal structure. One can see the formation of two strong hydrogen bonds between the amide group of Gln726 and the guanine group of the GMP molecule. In addition, the rest of the hydrogen-bonding network looks quite reasonable.

Binding free energy calculations were also performed on both the QM/MM-optimized structure while maintaining the original Gln726 position and the interchanged version for the PDE10−GMP system. The calculated binding free energy for the interchanged structure is ∼22 kcal/mol lower than the original one, as seen in Table 3. The significant energy decrease is mainly derived from two hydrogen bonds formed between the amide group of Gln726 and the guanine group of GMP. This confirms that the amide oxygen and nitrogen atoms in PDE10−AMP should be different from PDE10−GMP. As a result, PDE10 can hydrolyze both cAMP and cGMP primarily because Gln726 can flip the amide group and bind to both cyclic nucleotides.

Conclusion

Quantum mechanical/molecular mechanical (QM/MM) geometry optimization starting from the X-ray crystal structure have been performed to characterize the PDE10 structure and the state of the products AMP and GMP in the PDE10−AMP and PDE10−GMP complexes. All results suggest that there is only one phosphate oxygen atom (O1) protonated for both AMP and GMP molecules in the product complexes.

The conflict between the amide group of Gln726 and the guanine group of GMP in the X-ray crystal structure has been resolved by flipping the amide group of Gln726. As a result of the interchange of the amide nitrogen and oxygen atoms, two strong hydrogen bonds between the amide group of Gln726 and

TABLE 3: Energetic Considerations (kcal/mol) Obtained From the QM/MM-PBSA Calculations at $T = 298.15$ K and $P = 1$ atm for the GMP Binding with PDE10

	GMP (O1H,O3H)-flip-Glu726[a]	GMP (O1H,O3H)[b]
$\Delta E_{QM/MM}$(gas)	−206.6	−196.8
ΔG_{solv}	109	122.2
ΔE (bind) or ΔH	−97.6	−74.6
$-T\Delta S$	24.9	23.9
ΔG_{bind}(aq)	−72.7	−50.7
ΔG_{bind}^{rela}(aq)	0.0	22.0

[a] The charge on GMP = 0 with O1 and O3 protonated in the original file. The proton on the O3 atom migrated to the Oδ atom of Asp674 after QM/MM geometry optimization. O1 was protonated only after geometry optimization. The amide orientation of Glu726 was interchanged relative to the X-ray crystal structure. [b] The charge on GMP = 0 with O1 and O3 protonated in the original file. The proton on the O3 atom migrated to the Oδ atom of Asp674 after QM/MM geometry optimization. O1 was protonated only after geometry optimization. The original X-ray crystal structure amide orientation of Glu726 was maintained.

the guanine group of GMP are formed. Binding free energies were calculated for the QM/MM-optimized structures where in one case the amide position of Gln726 in the X-ray crystal structure was maintained and in the second case where the amide group is flipped in the PDE10−GMP system. The calculated binding free energy in the flipped case is ∼22 kcal/mol lower than the X-ray crystal structure. The significant energy decrease is derived mainly from the formation of two hydrogen bonds between the amide group of Gln726 and the guanine group of GMP. This implies that the amide oxygen and nitrogen atoms in PDE10−AMP are different from PDE10−GMP. Therefore, PDE10 can hydrolyze both cAMP and cGMP. Furthermore, our study concludes that the conformation of the amide oxygen and nitrogen atoms in PDE10−AMP is different from that in PDE10−GMP.

Acknowledgment. This research was supported by the NIH (grant RC1MH088480). The authors also acknowledge the Center for Computational Sciences (CCS) at the University of Kentucky for supercomputing time on IBM X-series Cluster with 340 nodes or 1360 processors.

References and Notes

(1) Callahan, S. M.; Cornell, N. W.; Dunlap, P. V. *J. Biol. Chem.* **1995**, *270*, 17627–17632.
(2) Conti, M.; Jin, S. L. C.; Monaco, L.; Repaske, D. R.; Swinnen, J. V. *Endocrin. Rev.* **1991**, *12*, 218.
(3) Houslay, M. D. *Semin. Cell Dev. Biol.* **1998**, *9*, 161–167.
(4) Conti, M.; Jin, S. L. C. *Prog. Nucleic Acid. Res.* **2002**, *63*, 1–38.
(5) Mehats, C.; Andersen, C. B.; Filopanti, M.; Jin, S. L. C.; Conti, M. *Trends Endocrin. Met.* **2002**, *13*, 29–35.
(6) Park, J. Y.; Richard, F.; Chun, S. Y.; Park, J. H.; Law, E.; Horner, K.; Jin, S. L. C.; Conti, M. *Mol. Endocrinol.* **2003**, *17*, 1117–1130.
(7) Zhang, H. T.; Steketee, J. D.; Jin, S. L. C.; Conti, M.; O'Donnell, J. M. *FASEB J.* **2003**, *17*, A206–A207.
(8) Houslay, M. D.; Adams, D. R. *Biochem. J.* **2003**, *370*, 1–18.
(9) Yamato, S.; Shoda, R.; Akiyama, J.; Uemura, N.; Tokuhara, M.; Shimizu, T.; Matsueda, K. *Gastroenterology* **2003**, *124*, A579–A579.
(10) Francis, S. H.; Turko, I. V.; Corbin, J. D. *Prog. Nucleic Acid Res. Mol. Biol.* **2001**, *65*, 1–52.
(11) Karnam, S. M.; Huiping, Z.; Gabriel, M. M. *Am. J. Physiol. Cell Physiol.* **2001**, *282*, C508–C517.
(12) Manganiello, V. *Mol. Pharmacol.* **2003**, *63*, 1209–1211.
(13) Fujishige, K.; Kotera, J.; Michibata, H.; Yuasa, K.; Takebayashi, S.; Okumura, K.; Omori, K. *J. Biol. Chem.* **1999**, *274*, 18438–18445.
(14) Soderling, S. H.; Bayuga, S. J.; Beavo, J. A. *Proc. Natl. Acad. Sci.* **1999**, *96*, 7071–7076.
(15) Loughney, K.; Snyder, P. B.; Uher, L.; Rosman, G. J.; Ferguson, K.; Florio, V. A. *Gene* **1999**, *234*, 109–117.
(16) Siuciak, J. A.; Chapin, D. S.; Harms, J. F.; Lebel, L. A.; McCarthy, S. A.; Chambers, L.; Shrikhande, A.; Wong, S.; Menniti, F. S.; Schmidt, C. J. *Neuropharmacology* **2006**, *51*, 386–396.
(17) Siuciak, J. A.; McCarthy, S. A.; Chapin, D. S.; Fujiwara, R. A.; James, L. C.; Williams, R. D.; Stock, J. L.; McNeish, J. D.; Strick, C. A.; Menniti, F. S.; Schmidt, C. J. *Neuropharmacology* **2006**, *51*, 374–385.
(18) Rodefer, J. S.; Murphy, E. R.; Baxter, M. G. *Eur. J. Neurosci.* **2005**, *21*, 1070–1076.
(19) Wang, H.; Liu, Y.; Hou, J.; Zheng, M.; Robinson, H.; Ke, H. *Prog. Nucleic. Acid. Res.* **2007**, *104*, 5782–5787.
(20) Zhang, K. Y.; Card, G. L.; Suzuki, Y.; Artis, D. R.; Fong, D.; Gillette, S. *Mol. Cell* **2004**, *15*, 279–286.
(21) Zoraghi, R.; Corbin, J. D. Francis, S.H. *J. Biol. Chem.* **2006**, *281*, 5553–5558.
(22) McDonald, I. K.; Thornton, J. M. *Protein Eng.* **1995**, *8*, 217–224.
(23) Hooft, R. W.; Sander, C.; Vriend, G. *Proteins* **1996**, *26*, 363–376.
(24) Word, J. M.; Lovell, S. C.; Richardson, J. S.; Richardson, D. C. *J. Mol. Biol.* **1999**, *285*, 1735–1747.
(25) Lovell, S. C.; Davis, I. W.; Arendall, W. B., III *Proteins* **2003**, *50*, 437–450.
(26) Higman, V. A.; Boyd, J.; Smith, L. J.; Redfield, C. *J. Biomol. NMR* **2004**, *30*, 327–346.
(27) Weichenberger, C. X.; Sippl, M. J. *Structure* **2006**, *14*, 967–972.
(28) Weichenberger, C. X.; Sippl, M. J. *Bioinformatics* **2006**, *22*, 1397–1398.
(29) Weichenberger, C. X.; Sippl, M. J. *Nucleic Acids Res.* **2007**, *35*, W403–W406.
(30) Wang, H.; Liu, Y.; Hou, J.; Chen, Y.; Robinson, H.; Ke, H. *J. Biol. Chem.* **2005**, *280*, 30949–30955.
(31) Zhang, Y.; Lee, T.; Yang, W. *J. Chem. Phys.* **1999**, *110*, 46–54.
(32) Zhang, Y. *J. Chem. Phys.* **2005**, *122*, 024114.
(33) Zheng, F.; Yang, W.; Ko, M.-C.; Liu, J.; Cho, H.; Gao, D.; Tong, M.; Tai, H.-H.; Woods, J. H.; Zhan, C.-G. *J. Am. Chem. Soc.* **2008**, *130*, 12148–12155.
(34) Liu, J.; Hamza, A.; Zhan, C.-G. *J. Am. Chem. Soc.* **2009**, *131*, 11964–11975.
(35) Xiong, Y., Liu, J., Yang, G., Zhan, C.-G. , *J. Comput. Chem.* **2010**, *31*, 1592−1602.
(36) Case, D. A.; Darden, T.; Cheatham, T. E., III; Simmerling, C.; Wang, J.; Duke, R. E.; Luo, R.; Merz, K. M.; Wang, B.; Pearlman, D. A.; Crowley, M.; Brozell, S.; Tsui, V.; Gohlke, H.; Mongan, J.; Hornak, V.; Cui, G.; Beroza, P.; Schafmeister, C.; Caldwell, J. W.; Ross, W. S.; Kollman, P. A. *AMBER 8*; University of California: San Francisco, CA, 2004.
(37) Becke, A. D. *J. Chem. Phys.* **1993**, *98*, 5648–5652.
(38) Lee, C.; Yang, W.; Parr, R. G. *Phys. Rev. B* **1988**, *37*, 785–789.
(39) Stephens, P. J.; Devlin, F. J.; Chabalowski, C. F.; Frisch, M. J. *J. Phys. Chem.* **1994**, *98*, 11623–11627.
(40) Hehre, W. J., Radom, L., Schleyer, P. R., Pople, J. A. *Ab Initio Molecular Orbital Theory*; John Wiley & Sons: New York, 1987.
(41) Frisch, M. J.; Trucks, G. W.; Schlegel, H. B.; Scuseria, G. E.; Robb, M. A.; Cheeseman, J. R.; Montgomery, J. A., Jr.; Vreven, T.; Kudin, K. N.; Burant, J. C.; Millam, J. M.; Iyengar, S. S.; Tomasi, J.; Barone, V.; Mennucci, B.; Cossi, M.; Scalmani, G.; Rega, N.; Petersson, G. A.; Nakatsuji, H.; Hada, M.; Ehara, M.; Toyota, K.; Fukuda, R.; Hasegawa, J.; Ishida, M.; Nakajima, T.; Honda, Y.; Kitao, O.; Nakai, H.; Klene, M.; Li, X.; Knox, J. E.; Hratchian, H. P.; Cross, J. B.; Adamo, C.; Jaramillo, J.; Gomperts, R.; Stratmann, R. E.; Yazyev, O.; Austin, A. J.; Cammi, R.; Pomelli, C.; Ochterski, J. W.; Ayala, P. Y.; Morokuma, K.; Voth, G. A.; Salvador, P.; Dannenberg, J. J.; Zakrzewski, V. G.; Dapprich, S.; Daniels, A. D.; Strain, M. C.; Farkas, O.; Malick, D. K.; Rabuck, A. D.; Raghavachari, K.; Foresman, J. B.; Ortiz, J. V.; Cui, Q.; Baboul, A. G.; Clifford, S.; Cioslowski, J.; Stefanov, B. B.; Liu, G.; Liashenko, A.; Piskorz, P.; Komaromi, I.; Martin, R. L.; Fox, D. J.; Keith, T.; Al-Laham, M. A.; Peng, C. Y.; Nanayakkara, A.; Challacombe, M.; Gill, P. M. W.; Johnson, B.; Chen, W.; Wong, M. W.; Gonzalez, C.; Pople, J. A. *Gaussian 03*, revision A.1; Gaussian, Inc.: Pittsburgh, PA, 2003.
(42) Gilson, M. K.; Sharp, K. A.; Honig, B. H. *J. Comput. Chem.* **1988**, *9*, 327–335.
(43) Jayaram, B.; Sharp, K. A.; Honig, B. H. *Biopolymers* **1989**, *28*, 975–993.
(44) Sanner, M. F.; Olson, A. J.; Spehner, J. C. *Biopolymers* **1996**, *38*, 305.
(45) Pan, Y.; Gao, D.; Zhan, C.-G. *J. Am. Chem. Soc.* **2008**, *130*, 5140–5149.

JP911527Y